

## Investigation of the functional capability of modified silicon-based photodiodes structure

Sh. B. Utamuradova <sup>a</sup>, F. A. Giasova <sup>b</sup>, M. S. Paizullakhanov <sup>c</sup>,  
S. Yu. Gerasimenko <sup>d</sup>, M. A. Yuldoshev <sup>e,g,\*</sup>, S. R. Boydedayev <sup>g</sup>,  
M. R. Bekchanova <sup>h</sup>

<sup>a</sup> *Institute of Semiconductor Physics and Microelectronics, National University of Uzbekistan, Uzbekistan*

<sup>b</sup> *Kimyo International University in Tashkent, Uzbekistan*

<sup>c</sup> *Institute of Materials Science of the Academy of Sciences of the Republic of Uzbekistan, Uzbekistan*

<sup>d</sup> *Physical-Technical Institute of the Academy of Sciences of the Republic of Uzbekistan, Uzbekistan*

<sup>e</sup> *Namangan State Pedagogical Institute, Uzbekistan*

<sup>g</sup> *Namangan State Technical University, Uzbekistan*

<sup>h</sup> *University of Public Security of the Republic of Uzbekistan, Uzbekistan*

Based on the experimental data, the results of the study of photoelectric and gain characteristics of modified multi-barrier photodiode Au-nCdS-nSi-pCdTe-Au structures are presented, which are obtained by the method of vacuum evaporation in a quasi-closed volume by sputtering cadmium sulfide and cadmium telluride layers on a silicon substrate with a specific resistance of 607.47 Ohm·cm. It is shown that the structures in the passing direction of the current at low illumination levels operate as injection photodiodes, and also the optical spectral range (0.3÷0.95 μm) covers from the nSi-pCdTe-Au side and (1.0÷1.4 μm) from the Au-nCdS-nSi side with a photosensitivity of 0.57 A/W at a wavelength of 1310 nm. In addition, the possibility of their application in optical power attenuation meters is considered.

(Received May 2, 2025; Accepted August 21, 2025)

**Keywords:** Photodiode, Structure, Heterojunction, Optical characteristics, Optical signal, Photosensitivity, Power, Meter, Attenuation

### 1. Introduction

Currently, intensive work is underway to develop new types of noiseless, highly sensitive photodetectors with internal amplification for detecting small optical signals, which is the main task of modern semiconductor optoelectronics [1-4]. High-quality reception of optical signals is possible under the condition of high sensitivity of receivers (photodiodes) of weak optical signals, which requires its own solution, since the currently used avalanche photodiodes cannot operate without stabilization of the operating mode, and in the avalanche mode, noise currents increase in them [5]. To eliminate noise currents, optoelectronic device developers began to turn to bipolar (n-p-n, p-n-p) and field-effect transistors with a control p-n junction, which have internal gain. However, in bipolar phototransistors, the effect of charge accumulation in the base and relatively large leakage currents of  $7 \cdot 10^{-5}$  A/cm<sup>2</sup> limit their use at low input signal levels [6, 7], since the useful signal must be much greater than the leakage current. In addition, the gain and photosensitivity in them are contradictory. An increase in the gain requires a decrease in the base thickness, and an increase in photosensitivity is achieved by increasing the base thickness. The resulting contradictions are problematic, that is, a bipolar phototransistor can have high

---

\* Corresponding author: [murod.yuldoshev1993@gmail.com](mailto:murod.yuldoshev1993@gmail.com)

<https://doi.org/10.15251/CL.2025.228.753>

photosensitivity or a high gain. The authors of the work [8–9], using these properties of field-effect and bipolar transistors, developed two- and three-barrier photodiode structures based on gallium arsenide with forward and reverse-connected junctions, in which one of the semiconductor junctions is replaced by a metal-semiconductor junction.

In addition, impurity photodetectors such as injection photodiodes with internal amplification, which are controlled by injection from contacts with high sensitivity in the spectral range from ultraviolet to far infrared region [10], are used to detect optical signals. Such photodiodes are created on the basis of many semiconductors (doped with germanium, silicon, gallium arsenide, indium antimonide, solid solutions of  $A^3B^5$  compounds and other materials) and their characteristics are studied in [11, 12].

There is information in the literature about injection photodiodes based on chalcogenide compounds, in particular based on cadmium sulfide [13] and telluride [14]. However, information about photodiodes based on the  $A^2B^6$  compound is insufficient. This is due to the labor-intensive process of obtaining p-type conductivity in such semiconductor materials, except for cadmium telluride, and the small value of the diffusion bias length of minority carriers. According to the authors [15, 16], a multifunctional photodiode can be created based on a semiconductor structure with  $A^2B^6$  heterojunctions, in which the counter currents of nonequilibrium carriers are regulated. Due to such regulation, an inversion of the photosensitivity sign occurs at different base thicknesses, which are sensitive to optical signals of the near ultraviolet, visible, and near infrared regions of the optical radiation spectrum. With a high base resistance of the structure, diffusion currents dominate in the current transfer and the photodiode has the property of internal amplification of the primary photocurrent.

Due to the improvement of optoelectronic devices for recording and processing optical signals, the requirement for the development of inertia-free, low-noise photodiodes that are stable, have low inertia, and have linear photoelectric characteristics is increasing [17]. Noise can be eliminated by implementing the photodiodes in a photovoltaic mode with a reduced reverse dark current and minimal inertia. A simple solution to these problems is the development of modified photodiodes with increased response speed based on high-grade silicon with an  $A^2B^6$  Schottky barrier, in which the counter currents of nonequilibrium carriers are regulated and there is no charge accumulation that leads to a decrease in barrier capacities [18, 19].

Recently, considerable attention has been paid to the creation of new types, improvement of existing ones and introduction into production of devices based on semiconductor compounds  $A^2B^6$  and their solid solutions [20, 21]. Since they are superior to devices based on silicon in some electrophysical and operational characteristics [14]. One of the promising materials from a series of  $A^2B^6$  compounds is cadmium telluride (CdTe) and cadmium sulfide (CdS). A large band gap and a high absorption coefficient characterize its semiconductor as an optimal photoconverter material [21] for creating photodetectors that record various optical signals [22] and detectors [23] of ionizing radiation.

This paper presents the results of a study of the optical-electrical characteristics of a multi-barrier thin-film photodiode nCdS-nSi-pCdTe structure with a heterojunction as an optical signal receiver and estimates its photoelectric gain.

## 2. Experimental samples and research methods

As is known, modern microelectronics and solid-state electronics solve the problems of reducing the material intensity of the technology for the production of devices and microcircuits by developing, mastering and implementing local methods for forming device structures [24]. The manufacturing technology and the main parameters of the multi-barrier photodiode nCdS-nSi-pCdTe structure are given in previously published works [25, 26].

Of considerable interest is the distribution of the current-voltage (CV) characteristic in multilayer structures at operating temperatures, which allow one to determine the non-ideality of the p-n junction and various parameters of semiconductor structures [27]. The current-voltage characteristics of the structure were recorded in the forward and reverse directions over wide

ranges of current and voltage changes. In previously published works [28, 29], a complete analysis of the CV of the nCdS-nSi-pCdTe photodiode structure is given.

The spectral characteristic of the photosensitive nCdS-nSi-pCdTe heterostructure was recorded at room temperature using an SPM-2 setup from Carl Zeiss Jena with a quartz prism. A Uniel 3200 K halogen lamp with a power of 100 W was used as a radiation source. The measurement range covered from 0.25 to 3  $\mu\text{m}$ , in which carrier excitation was ensured. The operating voltage was supplied from an Aleksadrit B5-43 power supply unit with a step of 0.1 V (Fig. 1).

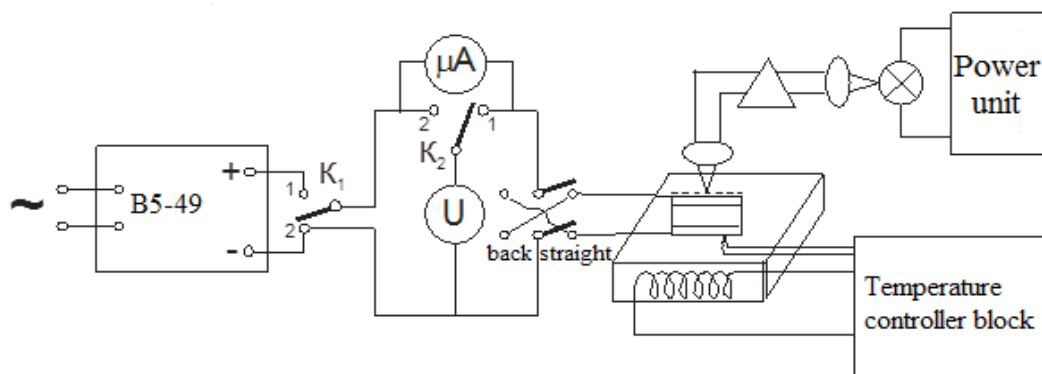


Fig. 1. Block diagram for measuring the temperature dependence of the volt-ampere and spectral characteristics of structures.

The sensitivity of the structures was determined in normalized units in the photodiode mode. The measurement data obtained at the lowest bias voltages, in particular at 0.05 to 0.5 V, were taken as the main curve. The photocurrent (the difference between the values of the light and dark currents) was determined at each wavelength. The normalizing (resulting in the same power) coefficient of the source was determined based on the bolometer data. When taking spectral characteristics in the photovoltaic mode, the short-circuit current is directly measured using an ammeter.

The current-voltage characteristics of photosensitive heterofilm CdS-nSi-CdTe structures under illumination were measured in both forward and reverse current directions at a room temperature of 20 °C (Fig. 2). The illumination level was maintained at  $E=0\div160$  lx. A specialized incandescent lamp SIRSh 6-100, with a power rating of 100 W and specifications comparable to those of a standard white light lamp, was used for the illumination of the structures. It is important to highlight that one lumen of electromagnetic radiation within the visible spectrum corresponds to a power of  $9.1\cdot10^{-3}$  W.

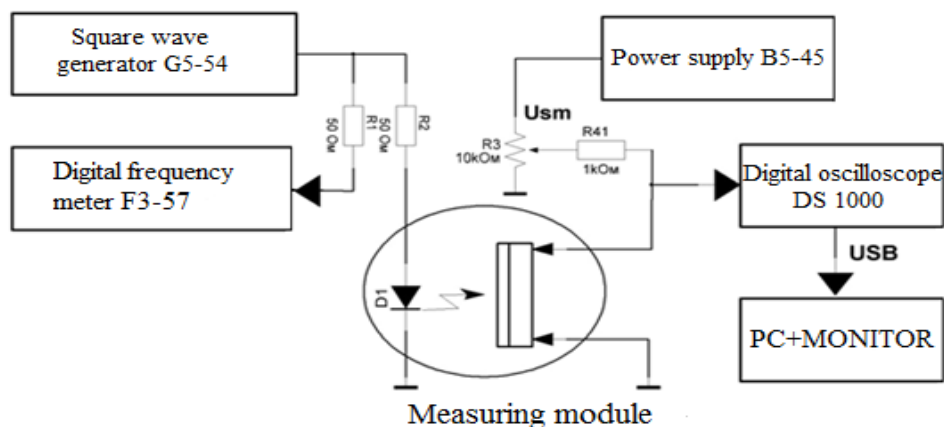


Fig. 2. Block diagram of measuring the light current-voltage characteristic with a DC bias.

### 3. Results and discussion

In the studied nCdS-nSi-pCdTe heterostructure [31], the relative spectral sensitivity, which is the spectral dependence of the photoresponse, allows us to describe the dependence of the photodetector output signal on the wavelength of the radiation incident on it. Studies of the spectral characteristics of the two-sided photosensitive multilayer nCdS-nSi-pCdTe structure with an area of 29 mm<sup>2</sup> showed that their optical spectral range  $\lambda=(0.3\div0.95\text{ }\mu\text{m})$  covers the nSi-pCdTe side and  $\lambda=(1.0\div1.4\text{ }\mu\text{m})$  on the nCdS-nSi side with characteristic features as shown in Fig. 3.

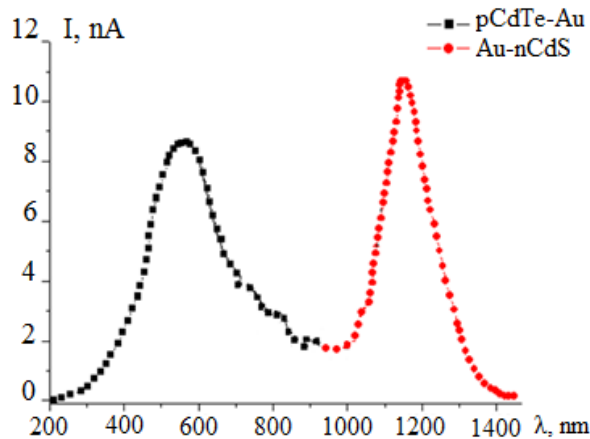


Fig. 3. Spectral characteristics of the nCdS-nSi-pCdTe structure under illumination from the side of the pCdTe-Au and Au-nCdS junctions.

In the nSi-pCdTe region with  $\lambda=(0.3\div0.95\text{ }\mu\text{m})$  the photocurrent curve ( $I_{ph}$ ) begins to increase sharply and reaches its maximum value  $I_{ph}=8.74\text{ nA}$  at  $\lambda\approx0.59\text{ }\mu\text{m}$ , then the photocurrent decreases sharply with further increase in the wavelength. In the nCdS-nSi region with  $\lambda=1.0\div1.4\text{ }\mu\text{m}$  it begins to increase sharply at a wavelength of 1.0  $\mu\text{m}$ , reaching its maximum value  $I_{ph}=10.7\text{ nA}$  at  $\lambda\approx1.23\text{ }\mu\text{m}$ , and then the photocurrent begins to decrease smoothly to  $\lambda\approx1.4\text{ }\mu\text{m}$ . From this it is evident that the nCdS-nSi-pCdTe structure has a wide range of spectral sensitivity  $\lambda=(0.3\div1.4\text{ }\mu\text{m})$ . In the first and second regions of the spectral distribution (Fig. 4), the photocurrent is of different polarities, which is due to the reverse inclusion of potential barriers between the Au-nCdS-nSi isotype junction and the nSi-pCdTe-Au heterojunction. In addition, the curve of the spectral distribution of photosensitivity shows that the isotype CdS-nSi heterojunction at the interface contains a low density of surface states. It follows from this that the structure has a rectification coefficient higher than two orders of magnitude and the appearance of a maximum on the curves  $I_{ph}(\lambda)$  at  $\lambda\approx0.59$  (1.23)  $\mu\text{m}$ , and the tangent part of the two curves along the decline in the long-wavelength region of the spectrum, corresponding to the width of the forbidden band of silicon.

Fig. 4 shows comparative spectral characteristics of the photosensitivity ( $S_\lambda$ ) dependences of silicon-based structures and photodiodes.

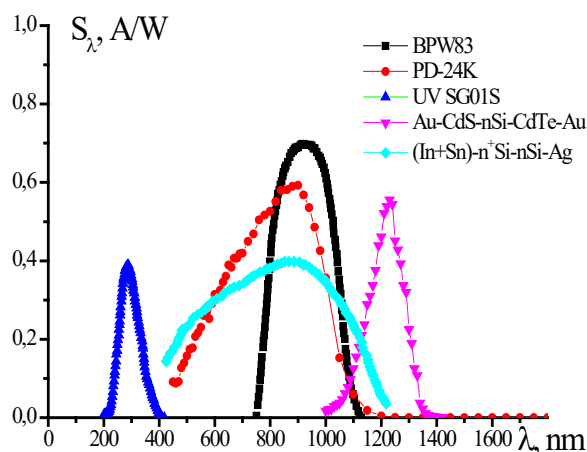


Fig. 4. Spectral characteristics of photosensitive structures based on silicon and photodiodes.

The appearance of the curves (Fig. 4) of the photosensitivity of the nCdS-nSi-pCdTe structure in the region of long wavelengths is practically no different from other photodiode structures, only the long-wave part of the spectral photosensitivity of the nCdS-nSi-pCdTe structure is extended towards the IR region of the spectrum, unlike other photodiodes with a photosensitivity power of 0.57 A/W [30].

Subsequently, the load current-voltage characteristics were examined under varying illumination intensities from the integrated source, peaking at  $\lambda=0.55 \mu\text{m}$ . This illumination was directed at both surfaces of the photosensitive nCdS-nSi-pCdTe structure, specifically when stimulated by light with energy exceeding the bandgap of the base region. The findings indicated that with an increase in illumination intensity, the relationship between the photocurrent and the operating voltage exhibits both linear and sublinear characteristics under reverse and forward voltage biases, as illustrated in Fig. 5.

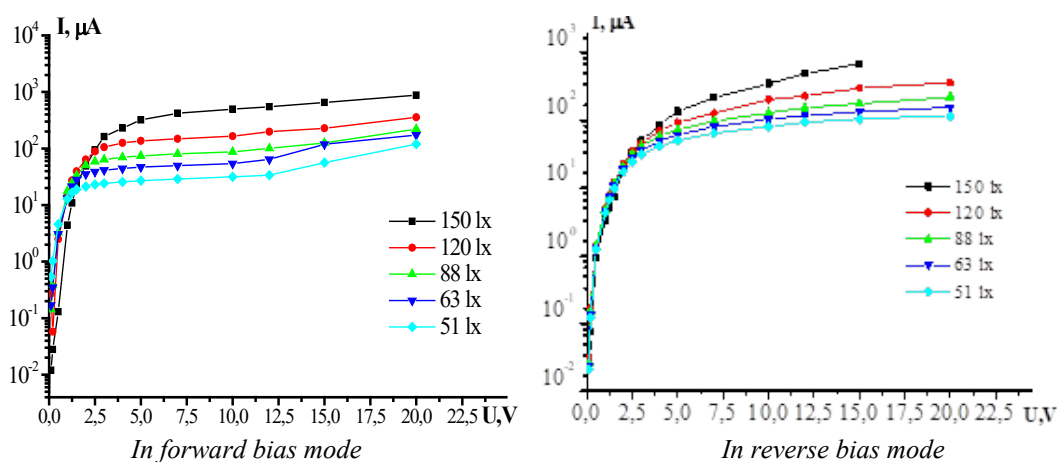


Fig 5. Current-voltage characteristic of the CdTe transition of the CdS-nSi-CdTe structure illuminated with light of different intensities.

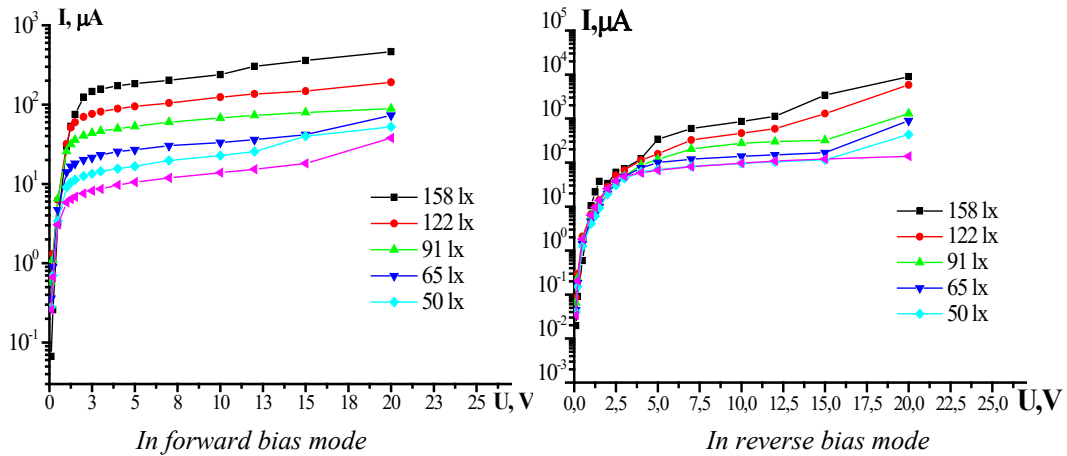


Fig 6. Current-voltage characteristic of the CdS transition of the CdS-nSi-CdTe structure illuminated with light of different intensities.

The load characteristics of the nCdS-nSi-pCdTe structures, illustrated in (Fig. 5 and Fig. 6), reveal a recurring pattern: multiple inflection points followed by saturation across all the curves. Notably, these inflection points consistently appear at similar power levels impacting the structure. The near-surface absorption of light within the semiconductor, coupled with the charge carrier separation driven by the electric field at the interface of the nSi-pCdTe or nCdS-nSi junction, results in noticeable changes in the response at low illumination intensities (0-90 lx). This behavior stems from the deeper layers of the heterostructure absorbing the more intense light (100-160 lx). The data show that the mechanisms of current flow in the dark and in the light are equally sublinear and only differ in the current value. In [31, 32], the authors found that when the structures operate in the double injection drift mode, the features of the bipolar drift of nonequilibrium carriers in the thickness of the n-base are of decisive importance, and the contribution of the injecting and accumulating contacts to this process is insignificant. In this structure, photoelectric injection current amplification is manifested, in which the base conductivity is determined by the modulation of mobility under the action of “impurity” illumination. [28, 33]. The significant increase in photocurrent observed at low input power levels stems from the charge carrier separation facilitated by the electric fields present within the nCdS-nSi-pCdTe multilayer heterostructures p-n and n-p junctions. Investigations of the inverse current-voltage relationship disclosed the dominance of thermionic currents within a specific current density range of approximately  $I \approx (1.3 \cdot 10^{-9} \div 1.1 \cdot 10^{-8} \text{ A/cm}^2)$ , accompanied by a photosensitivity of  $S_\lambda = 2.02 \cdot 10^{-4} \text{ A/W}$  [26].

The basic diagram of the reception and transmission of an optical signal using the example of an emitter - receiver is shown in Fig. 7. [34, 35], made on the basis of an experimental photodiode nCdS-nSi-pCdTe structure. According to the technical specifications, the laser diode used PL-DFB-1312-TO39 has a forward voltage of  $1.3 \div 2.0 \text{ V}$ , at a wavelength of 1312 nm, the maximum output radiation power is up to 30 mW, the width of the spectral line is  $< 2 \text{ MHz}$ .

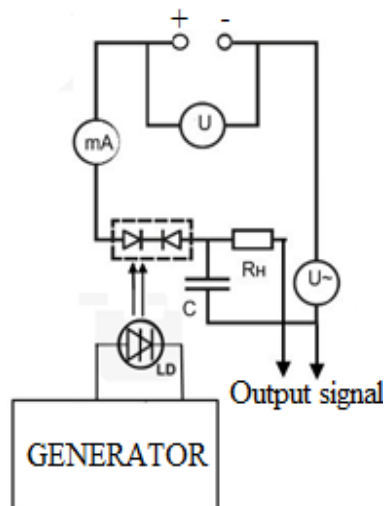


Fig. 7. Schematic diagram of optical reception of laser radiation by a photodiode.

The optical signal to the nCdS-nSi-pCdTe photodiode structure was supplied from a laser excited by a 200 Hz sinusoidal pulse generator. The optical-electrical characteristics of the emitter-receiver system are shown in Fig. 8, in which, without illumination, the dark current determined by the metal-semiconductor gate junction was 59.2 nA at a supply voltage of 50 V [28, 29].

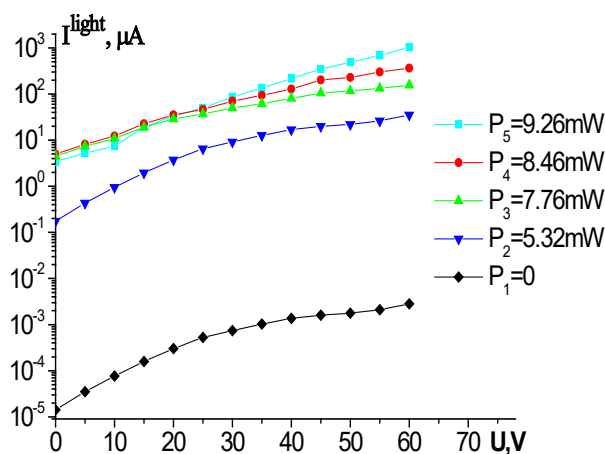


Fig 8. Output characteristics of the multi-barrier photodiode nCdS-nSi-pCdTe structure.

With laser irradiation, as the fixed values of radiation intensity increase, a family of output characteristics is formed (Fig. 8). Characteristic of the observed output characteristics is an increase in the light current with an increase in the operating voltage, while the dark current practically does not increase, that is, for a given intensity of laser radiation, we have an increase in the output signal. Current photosensitivity for a given intensity of laser radiation and the corresponding voltages is determined by the ratio of the output photocurrent to the value of the power of the light excitation signal [36]:

$$S_{U=V}^{\text{photo}} = \frac{I_{\text{output}}^{\text{photo}}}{P_n} \quad (1)$$

As follows from Fig. 8, the value of the output current photosensitivity will increase with the growth of the operating voltage, and accordingly, relative to the input (coming from the laser) light signal, we will have an amplified output signal. In this case, the input signal is taken to be the primary photocurrent created at an operating voltage equal to the contact potential difference of the illuminated junction, when the amplification has not yet occurred. The amplification of the primary photocurrent is due to the modulation of the bipolar drift mobility during irradiation with low-power “impurity” light. The input current photosensitivity, determined by the ratio of the photocurrent to the incoming power has its own values for each laser radiation intensity.

$$S_{\text{input}}^{\text{photo}} = \frac{I_{\text{input}}^{\text{photo}}}{P_n} \quad (2)$$

The conductivity of the base in the structure is determined by the injected carriers from the contacts, the current amplification is determined by the modulation of mobility under the influence of “impurity” illumination. In the amplification of the primary photocurrent on the sublinear section of the output characteristic (IV) (Fig. 8), an important role is played by the increase in the value of the bipolar drift velocity of nonequilibrium current carriers.

For the given electrical circuit for switching on a photodiode (Fig. 7), the gain will be determined by the ratio of the output signal to the input signal, that is, the ratio of the output current photosensitivity to the input current photosensitivity.

$$M_I = \frac{S_{U=V}^{\text{photo}}}{S_{\text{input}}^{\text{photo}}} \quad (3)$$

Experimentally obtained calculated data for the current gain coefficient based on the curves shown in Fig. 9.

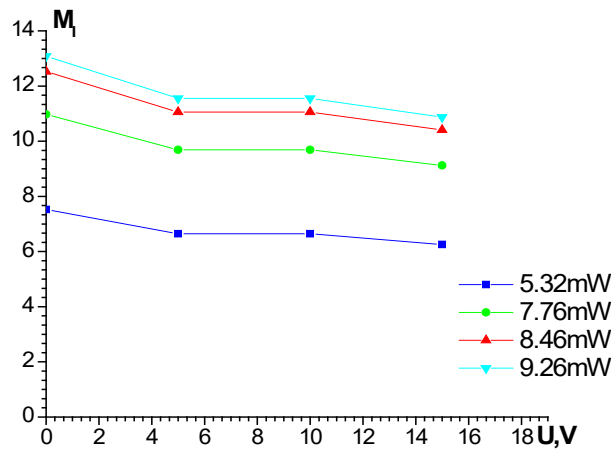


Fig. 9. Dependences of the current gain on the operating voltage at different light signal powers.

As can be seen from Fig. 9, the current gain decreases with increasing operating voltage, and an increase in the intensity of the light signal leads to an increase in its magnitude, i.e. the studied structure nCdS-nSi-pCdTe structure is effective for receiving weak optical signals (Fig. 9). Regarding the output voltage, it should be noted that it, being the product of photosensitivity and load resistance, has a greater value, the greater the output dynamic resistance.

$$S_{\text{output}}^{\text{photo}} = \frac{I_{\text{input}}^{\text{photo}}}{P_n} R_{\text{eq}}, \quad (4)$$



where,  $R_{eq}$  is the equivalent load

$$R_{eq} = \frac{R_{din}R_{load}}{R_{din}+R_{load}}, \quad (5)$$

$$R_{din} = \frac{\partial U_{output}}{\partial I_{output}}, \quad (6)$$

At a low power of 5.32 mW of the laser beam, the photosensitivity at 60 V reaches a maximum of 22 mA/W, after which, with an increase in the bias voltage, the current in the photodiode circuit begins to decrease sharply and changes its direction. This behavior of photosensitivity is due to an increase in the injection current in the junctions. In this case, the dependence (Fig. 9) has sections of rise and fall, which are associated with recombination processes at the boundary of the layers of the isotype heterojunction (nCdS-nSi). At high energies of laser irradiation, there is no change in the sign of the current in the photodiode circuit - the higher the laser irradiation energy, the lower the photosensitivity values. In addition, at high bias voltages, the proportion of photocarriers separated by the rear barrier (pCdTe-Au heterojunction) becomes decisive. In this case, the directions of the photocurrent and injection current in the structure coincide, which is confirmed by the experiment.

Consequently, internal amplification occurs in the structure and the most important indicator is its photosensitivity value, which is much greater than the photosensitivity of conventional silicon-based photodiodes. It should be noted that at a laser beam power of 9.26 mW, the photosensitivity is 106 mA/W at  $U=60$  V. This indicates that a redistribution of the potential between the front barrier and the base of the structure occurs, as a result of which additional carrier injection and internal amplification of the photocurrent occur.

Consideration of the gain of a field-controlled photodiode requires the use of the dependence of the volume charge layer thickness on the operating voltage and the processes of carrier photogeneration. As can be seen from the output characteristics (Fig. 8) of the photodiode structure, the photocurrent, i.e. the rate of carrier photogeneration, increases proportionally to the operating voltage. Accordingly, the main mechanism of photocurrent amplification is associated with the generation of minority photocarriers mainly in the volume charge layer [37], namely, dark carriers are transferred through the forward-connected junction in proportion to the number of carriers photogenerated in the turn-off junction. The relationship between the gain and the operating voltage can be linked through the volume charge layer by the following empirical expression:

$$M = \frac{I_{photo}}{I_{prim}} = \left( \frac{W^{work}}{W^{start}} \right)^n, \quad (7)$$

where,  $n$  is determined by the regularity of the dependence of the space charge layer on the voltage.

In this case, depending on the switching mode, the metal-semiconductor or semiconductor junctions alternately act as a gate controlling the thickness of the space charge layer, and the intensity of the incident light acts as a gate voltage. The photodiode structure has the quality of an amplifier, in which small changes in the input signal cause large changes in the output signal. The value of the output current photosensitivity will increase with an increase in the operating voltage, and accordingly, relative to the input (coming from the laser) light signal (amplified output signal). As a result, with the help of such photodiodes, it becomes possible to create optoelectronic devices for receiving and transmitting weak optical signals.

As is known, the input element for the development of a photodetector (photodiode) of the near IR range of optoelectronic devices are photodiode semiconductor structures. The proposed photodiode nCdS-nSi-pCdTe structure as a photodetector was used in an optical power attenuation meter designed for diagnostics of fiber-optic connections, that is, for solving complex and

important problems during the installation and technical operation of fiber-optic paths and connections [38,39].

#### 4. Conclusion

The experiments show that the modified nCdS-nSi-pCdTe photodiode structures have the quality of an amplifier, in which small changes in the input signal cause large changes in the output signal and are distinguished by two-sided sensitivity at both polarities of the operating voltage. In a wide operating spectral range ( $0.3\div 1.4$ )  $\mu\text{m}$ , the photoresponse in this system is due to direct optical excitation of carriers in the bulk of the films of  $\text{A}^2\text{B}^6$  compounds and the participation of states at the heterointerface or defects of the crystal structure of the silicon structure. In addition, at current densities of  $(1.3\cdot 10^{-9}\text{--}1.1\cdot 10^{-8})$   $\text{A}/\text{cm}^2$ , thermionic currents flow in the structure at an illumination value of 0.1 lx and a photosensitivity of  $2.02\cdot 10^{-4}$   $\text{A}/\text{W}$ , the illuminated surface of the structure with 0.55  $\mu\text{m}$ , which are accompanied by a mechanism of amplification of the primary photocurrent determined by the modulation of the ambipolar mobility of carriers. Compared to analogs, the created photodiode has increased functional characteristics.

Based on the created photodiode structure, a photodetector (photodiode) was developed and installed in an optical power meter to measure the average power of continuous optical radiation in fiber-optic communication lines.

#### References

- [1] I.D. Anisimova, I.M. Vikulin, F.A. Zaitov, Sh.D. Kurmashev, Semiconductor photodetectors, edited by V. I. Stafeev. Radio and Communications, 1984, ch. 101 p.
- [2] Sh.B. Utamuradova, Z.T. Azamatov, A.I. Popov, M.R. Bekchanova, M.A. Yuldoshev, A.B. Bakhromov, East Eur. J. Phys. 3, 278 (2024); <https://doi.org/10.26565/2312-4334-2024-3-27>
- [3] M.A. Yuldoshev, Z.T. Azamatov, A.B. Bakhromov, M.R. Bekchanova, East Eur. J. Phys. 4, 250 (2024); <https://doi.org/10.26565/2312-4334-2024-4-25>
- [4] S. Collin, F. Pardo, S.V. Averin, N. Bardo, J.-L. Pelar, Quantum Electronics. 2010, 40, No.5, pp.421-424; <https://doi.org/10.1070/QE2010v040n05ABEH014269>
- [5] R.L. Freeman, Fiber-optic communication systems. Moscow: Tekhnosfera, 2007, 514 p.
- [6] F.A. Giasova, M.A. Yuldoshev, Chalcogenide Letters, Vol.22, No.2, February 2025, p.123-129; <https://doi.org/10.15251/CL.2025.222.123>
- [7] S. Rakhmanov, K. Matchonov, H. Yusupov, K. Nasriddinov, D. Matrasulov, The European Physical Journal B. February 2025, Vol. 98, art.num.35; <https://doi.org/10.1140/epjb/s10051-025-00885-7>
- [8] A.V. Karimov, Three-barrier photodiode of Karimov, Author's certificate No.167399 of May 8, 1991.
- [9] A.B. Каримов, D.M. Yodgorova, F.A. Giasova, O.A. Abdulkhaev, International Journal of Advanced Science and Technology. 2020, vol. 29, No.9s, pp. 6350-6356.
- [10] Z.T. Azamatov, Sh.B. Utamuradova, M.A. Yuldoshev, N.N. Bazarbaev, East Eur. J. Phys. 2023, (2), pp. 187-190; <https://doi.org/10.26565/2312-4334-2023-2-19>
- [11] K. Xua, H.Y. Wangb, E.L. Chenc, S.X. Sunc, H.L. Wanga, H.Y. Meic, Journal of Ovonic Research, May - June 2024, Vol.20, No.3, pp. 395 – 403; <https://doi.org/10.15251/JOR.2024.203.395>
- [12] Ala'eddin A. Saif, A. Mindil, Journal of Ovonic Research, Vol. 20, No.4, July - August 2024, pp. 569 – 577; <https://doi.org/10.15251/JOR.2024.204.569>
- [13] I.M. Koldayev, V.V. Losev, B.M. Orlov, FTP 1984. Vol.18. 1316 p.
- [14] Sh.A. Mirsagatov, A.K. Uteniyazov, Letters to the Journal of Technical Physics. 2012, Vol.38, issue 1, pp. 70-76; <https://doi.org/10.1134/S1063785012010099>

- [15] I.B. Sapaeva, Sh.A. Mirsagatovb, B. Sapaevc and M.B. Sapaevb, *Inorganic Materials*, 2020, Vol.56, No.1, pp. 7-9; <https://doi.org/10.1134/S002016852001015X>
- [16] Sh.A. Mirsagatov, I.B. Sapaev, Sh.R. Valieva and D. Babajanov, *Journal of Nanoelectronics and Optoelectronics*, 2014, Vol.9, pp.1-10; <https://doi.org/10.1166/jno.2014.1685>
- [17] Elia Scattolo, Alessandro Cian, Luisa Petti, Paolo Lugli, Damiano Giubertoni, Giovanni Paternoster, *Sensors (Basel)*, 2023 Jan 11,23 (2); <https://doi.org/10.3390/s23020856>
- [18] F. Sakera, L.Remachea, D. Belfennacheb, K.R. Cheboukia, R. Yekhlef, *Chalcogenide Letters*. Vol.22, No.2, February 2025, pp. 151 – 166; <https://doi.org/10.15251/CL.2025.222.151>
- [19] K. Kannan, B. Manjunatha, T. Marimuthu, P. Sangeetha, *Chalcogenide Letters*. Vol.22, No.2, February 2025, p. 167 – 175; <https://doi.org/10.15251/CL.2025.222.167>
- [20] T.M. Razykov, A. Bosiob, B. Ergashev, K.M. Kouchkarov, A. Romeoc, N. Romeob, R. Yuldoshov, M. Baiev, M. Makhmudov, J. Bekmirzoyev, R. Khurramov, E. Fazylov, *Solar Energy*, 193 (15), 519 (2019); <https://doi.org/10.1016/j.solener.2019.09.072>
- [21] Jose G. Rocha, Senentxu Lanceros-Mendez. *Recent Patents on Electrical Engineering*, 4 (1) 1-26. (2011); <https://doi.org/10.2174/1874476111104010016>
- [22] M.A. Yuldoshev, *Physics AUC*, vol. 34, 2024, pp. 192-197; [http://cis01.central.ucv.ro/pauc/vol/2024\\_34/15\\_PAUC\\_2024\\_192\\_197.pdf](http://cis01.central.ucv.ro/pauc/vol/2024_34/15_PAUC_2024_192_197.pdf)
- [23] A.S. Achilov, Sh.A. Mirsagatov, *PSE*, 2015, vol.13, No.3
- [24] V.A. Bespalov, N.A. Dyuzhev, V.Yu. Kireev, *Russian Nanotechnologies*, 2022, Vol.17, No.1, pp. 29-45; <https://doi.org/10.1134/S2635167622010037>
- [25] F.A. Giasova, *Semiconductor Physics*. 19 January 2024, 55 p
- [26] Sharifa Utamuradova, Khojakbar Daliev, Shakhrukh Daliev, Sultanpasha Muzafarova, Kakhramon Fayzullaev, Gulnoza Muzafarova. *E3S Web of Conferences* 583, 04006 (2024) ITESE-2024; <https://doi.org/10.1051/e3sconf/202458304006>
- [27] S.I. Rambeza, *Methods of measuring the main parameters of semiconductors: Textbook. Manual*. Voronezh: VSU, 1989. 224 p.
- [28] F.A. Giasova, A.Z. Rakhmatov, K. Amonov, *Development of modern science and education: analysis of experience and trends. Collection of articles of the International scientific and practical conference held on December 5, 2022 in Petrozavodsk*. pp. 289-295.
- [29] Sharifa B. Utamuradova, Khodjakbar S. Daliev, Shakhrukh Kh. Daliev, Sultanpasha A. Muzafarova, Kakhramon M. Fayzullaev, Gulnoza A. Muzafarova. *East European Journal of Physics*. 4. 256-261 (2024); <https://doi.org/10.26565/2312-4334-2024-4-26>
- [30] F.A. Giasova, *Physics of semiconductors and microelectronics*, 2022, volume 4, issue 1, pp. 42-50.
- [31] P.M. Karageorgii-Alkalaev, A.Iu. Leiderman, *Photosensitive semiconductor structures with deep impurities*. Tashkent, «FAN» 1981. 200 p.
- [32] M. Akramov, C. Trunk, J. Yusupov and D. Matrasulov, *EPL*, 147 (2024) 62001; <https://doi.org/10.1209/0295-5075/ad752e>
- [33] B.M. Garin, V.I. Stafeev, *Sbornik trudov MFTI. Ser. Radiotekhnika i elektronika (Collection of papers of MIPT. Ser. Radiotechnics and electronics)*. Moscow, MFTI. 1972. vol.2. 88 p.
- [34] A.S. Aleinik, E.V. Vostrikov, S.A. Volkovsky, I.G. Deineka, V.E. Strigalev, I.K. Meshkovsky, *Fundamentals of circuit design of transceiver electronic devices: tutorial*. - St. Petersburg: ITMO University, 2021, 149 p.
- [35] D.M. Yodgorova, F.A. Giasova, R.G. Zakirov, *Computational nanotechnology*, 2-2018, pp. 87-90.
- [36] A.N. Ignatov, *Optoelectronic devices and equipment*. Moscow: Eco-Trends, 2006. 272 p.
- [37] M. Koussour, S. Bekovb, J. Rayimbaev, A. Syzdykova, S. Muminovd, I. Ibragimov, *Physics of the Dark Universe* 47 (2025) 101799; <https://doi.org/10.1016/j.dark.2024.101799>
- [38] F.A. Giasova, A.Z. Rakhmatov, R.G. Zakirov, D.M. Yodgorova, *European Journal of*

Technical and Natural Sciences. Scientific journal. 2022, No.6, pp. 97-102;

<https://doi.org/10.29013/EJTNS-22-6-97-102>

[39] R.G. Zakirov, F.A. Giasova, Safety in Aviation and Space Technologies, Lecture Notes in Mechanical Engineering. 2022, pp.23-32;

[https://doi.org/10.1007/978-3-030-85057-9\\_3](https://doi.org/10.1007/978-3-030-85057-9_3)